

Effect of Different Representations of Wind Turbines on the SSR Analysis in the Double Cage Induction Generator Based Wind Farm

Mohammad Kazem Salehi¹ and Roohalamin Zeinali Davarani^{2,†}

^{1,2} Department of Electrical Engineering, Faculty of Electrical and Computer Engineering, Graduate University of Advanced Technology, Kerman, Iran

A In this paper different representations of a wind farm based on double-cage induction generators connected to a
B series-compensated line is studied and their effect on the Subsynchronous Resonance (SSR) is analyzed. For this purpose,
S three representation types of wind turbines in SSR studies of the wind farm are considered as 1) Single Turbine
T Representation (STR), 2) Multiple Turbine Representation (MTR), and 3) Full Turbine Representation (FTR). To select the
R acceptable representation of the wind farm in SSR analysis, the wind farm is modeled by three representation and the test
A system eigenvalues are obtained for different conditions of the power system and the results are compared together. For
C this purpose, three scenarios are considered. In the first and second scenarios, all of the Wind Turbine Generators (WTGs)
T have identical electrical and mechanical parameters but WTGs in the third scenario are different. In the first scenario, all
wind turbines are subjected to the same wind speed, and in the second and third scenarios, each group of wind turbines is
subjected to the same wind speed. In addition, the analytical results are validated by electromagnetic transient simulation
using PSCAD/EMTDC software.

Article Info

Keywords:

Double cage induction generator,
Sub-synchronous resonance, Wind power plant,
Wind turbine representation

Article History:

Received 2018-12-02
Accepted 2019-05-17

I. INTRODUCTION

Worldwide, the installed capacity of wind power plants is increasing rapidly. Technological advancements, design improvements, and costs reduction have played a significant role in increasing wind farms penetration levels in power system [1]. Many countries are going to generate 20% of their energy from renewable energy sources until 2020, which wind energy is recognized as the prime renewable source [2], [3]. The large power plants connecting to transmission and distribution networks have several basic problems [4-7]. Large wind farms are typically located in remote areas with a good wind pattern, which causes the

construction of long transmission line and consequently reduces transmission power [8], [9]. Different methods have been proposed to overcome this problem. One of these ways is the need for installing the new transmission lines, which isn't generally economic. Using the series compensation based series capacitors is another method, which enhances the power transfer capability with the existing transmission lines. Hence, it is being increasingly considered for large wind power plants [10-13]. Furthermore, using the series capacitors in the power network lines near to wind plants may also potentially cause SSR in the wind turbine induction generators [14]. In order to model the wind farm to study the dynamic behavior of the power system, a large number of papers have used the aggregated equivalent model [5], [11], [15], [16]. However, modeling the large number of Induction Generators (IGs) in a wind farm by a single equivalent IG may not be accurate, but papers that have analyzed the SSR

[†]Corresponding Author: r.zeinali@kgut.ac.ir
Tel: +98-3431623445, Fax: +98-3431623445
Faculty of Electrical and Computer Engineering, Graduate University of Advanced Technology, Kerman, Iran

in the wind farms have considered only the aggregated model for wind farms [10], [11], [18-28]. In addition, in the previous studies, it was assumed that all wind farms are connected at the same collector bus (an aggregated wind farm connected to a series compensated transmission line) [29-32]. In [33], to reduce the interaction between DFIG controllers and series capacitor a control criteria is explored. In [34], to investigate the effect of random wind speed on SSR analysis of DFIG a probabilistic method is proposed to assess the probabilistic stability of SSR. In [35], the authors review the articles related to the SSR analysis in the wind farm.

In this paper for different representations of wind turbines a comprehensive analysis of SSR potential in the DCIG based wind farm connected to a series compensated line is presented and the results are compared with each other. Furthermore, this paper present the potential of SSR in a realistic wind farm split into different clusters connected by cables and connected to a series-compensated line. For this purpose, Single Turbine Representation (STR), Multiple Turbine Representation (MTR) and Full Turbine Representation (FTR) are considered to modeling the wind turbines in SSR analysis of DCIGs. In STR, the wind farm is modeled by only a single wind turbine. In MTR, based on the wind turbines characteristics and received wind speed the wind farm is modeled by multi-wind turbines. In FTR, all of the wind turbines are separately considered in the modeling of the wind farm. To study the effect of wind farm representation on SSR phenomenon the eigenvalue analysis is carried out by the linear modal method through MATLAB software, which is validated with electromagnetic transient simulation studies using PSCAD/EMTDC. The paper is organized as follow:

The effect of series compensated transmission lines on power system stability is studied in section II. In section III the modeling of a wind farm based DCIG connected to a series compensated transmission line is presented. The obtained results from SSR analysis for different wind turbine representation are shown in section IV. Time domain simulation results are presented in Section V. Finally, Section VI concludes the paper.

II. EFFECT OF SERIES COMPENSATED TRANSMISSION LINES ON POWER SYSTEM STABILITY

The power system with series compensated transmission lines can be faced with Subsynchronous Resonance (SSR). The SSR phenomenon may affect the stability of the power system by i) Self-excitation due to induction generator effect (also called IGE) ii) Subsynchronous Torsional Interaction (also called SSTI), and iii) Transient torque (also called transient SSR) [10]. In this paper, all three aspects are considered. Eigenvalue analysis is extensively utilized for the

study of torsional interaction and induction generator effect. Transient torque study is done through the electromagnetic transient simulation in PSCAD/EMTDC software. For the IGE and SSTI analysis, subsynchronous and torsional modes are of interest. The variation of Subsynchronous and the torsional modes, respectively, used to study the induction generator effect and the torsional interaction.

III. SYSTEM MODELING

The study system is shown in Fig. 1. The study system includes a large wind farm based on double-cage induction generators (DCIG), which is connected to an infinite bus through a long distance series-compensated transmission line. The wind farm split into different clusters connected by cables (impedances). The single line diagram of the wind farm is shown in Fig. 2.

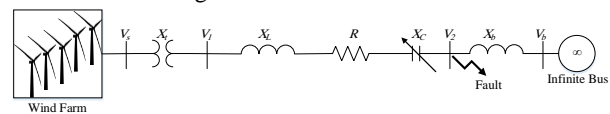


Fig. 1. Study system.

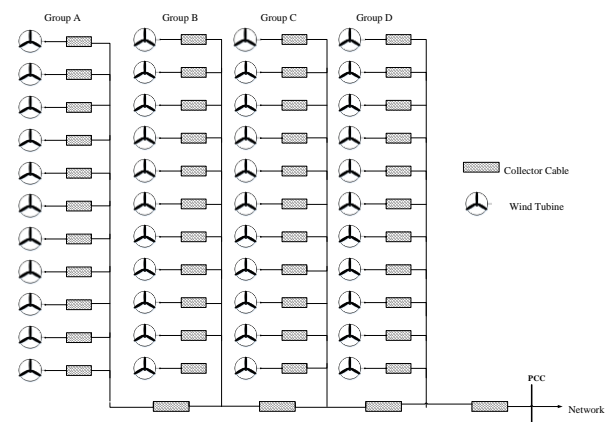


Fig. 2. Single line diagram of the wind farm.

In the following, the differential equations of the system are extracted.

A. WTG Torsional System Model

In order to investigate the SSR phenomenon, the turbine-generator is modeled as multi-mass. In this paper, a two-mass WTG drive train model, which shown in Fig. 3, is used. Dynamic equations of turbine generator shaft are expressed as (1)-(3) [11].

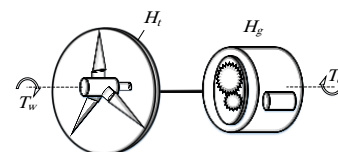


Fig. 3. Two-mass drive train model.

$$2H_t \frac{d}{dt} \omega_t = T_w - K_{ig} \delta_{ig} - D_{ig} (\omega_t - \omega_g) \quad (1)$$

$$\frac{d}{dt} \delta_{ig} = \omega_t - \omega_g \quad (2)$$

$$2H_g \frac{d}{dt} \omega_g = K_{ig} \delta_{ig} + D_{ig} (\omega_t - \omega_g) - T_e \quad (3)$$

In Eqs (1)-(3), ω_t and ω_g is the angular speed of the wind turbine and the generator, respectively, H_t and H_g is the inertia constant of wind turbine and generator, respectively, K_{ig} is the shaft stiffness between wind turbine and generator, δ_{ig} is the torsional angle between the wind turbine and generator, D_{ig} is the damping coefficient between the wind turbine and generator, T_w is the mechanical torque, and T_e is the electromagnetic torque.

B. Double cage induction generator model

Many wind farms in the world are based on the fixed speed turbine generators. For example the Brahmanvel wind farm with capacity of 550 MW in India, Twin Groves wind farm with capacity 396 MW in Illinois, Maple Ridge wind farm with capacity 322 MW in New York, Pioneer Prairie wind farm with capacity 302 MW in Iowa and Fowler Ridge wind farm with capacity 300 MW in Indiana used fixed speed wind turbines based squirrel cage induction generator [36].

A fixed-speed wind turbine generator consists of a conventional squirrel cage induction generator that is directly connected to the grid. The slip of the induction generator varies with the power generated. However, the variations are within 1%-2% of the rated generator speed. In this type of generator, since the rotor speed cannot be controlled, variation in the wind speed causes fluctuation in the input torque that is directly translated into variable output power. The induction generator output power increases with the increase in the torque applied to its shaft by the turbine. The stand-alone fixed speed induction generators do not produce reactive power. Therefore, an external source of reactive power such as capacitor bank should be used at the generator terminal. Fixed speed induction generators are designed as a single-cage rotor or double-cage rotor, but normally the squirrel cage induction generators with rated power above 5 kW are designed by the double-cage rotor. The steady-state equivalent circuit of a DCIG equipped by capacitor bank is shown in Fig. 4. The differential equations of the DCIG in the synchronously rotating d-q reference can be extracted as (4)-(9) [37]. In addition, the induction generator flux linkage (λ) and electromagnetic torque equations, respectively, are shown as (10) and (11) [11].

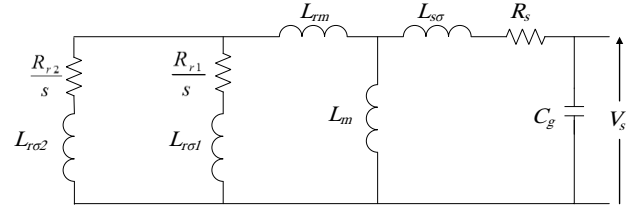


Fig. 4. The Steady-state equivalent circuit of a DCIG with a capacitor bank

$$\frac{d}{dt} \lambda_{ds} = -R_s I_{ds} + \omega_s \lambda_{qs} - V_{ds} \quad (4)$$

$$\frac{d}{dt} \lambda_{qs} = -R_s I_{qs} - \omega_s \lambda_{ds} - V_{qs} \quad (5)$$

$$\frac{d}{dt} \lambda_{dr1} = -R_{r1} I_{dr1} + s \omega_s \lambda_{qr1} \quad (6)$$

$$\frac{d}{dt} \lambda_{qr1} = -R_{r1} I_{qr1} - s \omega_s \lambda_{dr1} \quad (7)$$

$$\frac{d}{dt} \lambda_{dr2} = -R_{r2} I_{dr2} + s \omega_s \lambda_{qr2} \quad (8)$$

$$\frac{d}{dt} \lambda_{qr2} = -R_{r2} I_{qr2} - s \omega_s \lambda_{dr2} \quad (9)$$

$$\begin{bmatrix} \lambda_{ds} \\ \lambda_{qs} \\ \lambda_{dr1} \\ \lambda_{qr1} \\ \lambda_{dr2} \\ \lambda_{qr2} \end{bmatrix} = \begin{bmatrix} L_s & 0 & L_m & 0 & L_m & 0 \\ 0 & L_s & 0 & L_m & 0 & L_m \\ L_m & 0 & L_{r1} & 0 & L_{12} & 0 \\ 0 & L_m & 0 & L_{r1} & 0 & L_{12} \\ L_m & 0 & L_{12} & 0 & L_{r2} & 0 \\ 0 & L_m & 0 & L_{12} & 0 & L_{r2} \end{bmatrix} \begin{bmatrix} I_{ds} \\ I_{qs} \\ I_{dr1} \\ I_{qr1} \\ I_{dr2} \\ I_{qr2} \end{bmatrix} \quad (10)$$

$$L_s = L_{s\sigma} + L_m, L_{r1} = L_{r1\sigma} + L_{12}$$

$$L_{r2} = L_{r2\sigma} + L_{12}, L_{12} = L_m + L_m$$

$$T_e = L_m [I_{ds} (I_{qr1} + I_{qr2}) - I_{qs} (I_{dr1} + I_{dr2})] \quad (11)$$

Where, ω_s is the synchronous frequency (rad/s); V_{ds} and V_{qs} , I_{ds} and I_{qs} , are the d-q axis voltage and stator current of DCIG respectively; I_{dr1} and I_{qr1} , I_{dr2} and I_{qr2} are respectively the d-q axis current of first and second rotor cage; R_s and $L_{s\sigma}$ respectively are the resistance and leakage inductance of stator winding; R_{r1} and R_{r2} , $L_{r1\sigma}$ and $L_{r2\sigma}$ are the resistance and leakage inductance of first and second rotor cage respectively; L_m is the magnetizing inductance and, L_{12} is the mutual leakage inductance between two rotor cages.

C. Transmission line model

The differential equations of the transmission line can be extracted in the d-q reference by the equations (12)-(17) [11].

$$C_g \frac{d}{dt} V_{ds} = I_{ds} - I_d + \omega_s C_g V_{qs} \quad (12)$$

$$C_g \frac{d}{dt} V_{qs} = I_{qs} - I_q - \omega_s C_g V_{ds} \quad (13)$$

$$L \frac{d}{dt} I_d = V_{ds} - R I_d + \omega_s L I_q - V_{cd} - V_{bd} \quad (14)$$

$$L \frac{d}{dt} I_q = V_{qs} - R I_q - \omega_s L I_d - V_{cq} - V_{bq} \quad (15)$$

$$C \frac{d}{dt} V_{cd} = I_d + \omega_s C V_{cq} \quad (16)$$

$$C \frac{d}{dt} V_{cq} = I_q - \omega_s C V_{cd} \quad (17)$$

Where, V_{cd} and V_{cq} , V_{bd} , and V_{bq} , I_d and I_q are respectively the voltage across the series capacitor, infinite bus voltage, and the transmission line current in the d-q reference frame. C and C_g are respectively, the series capacitor of the transmission line, and the shunt capacitor bank at the terminal of the wind plant. In addition, L is defined as (18):

$$L = L_L + L_T + L_b \quad (18)$$

Where, L_L , L_T , and L_b , respectively are the inductance of the transmission line, the transformer, and infinite bus source.

D. Equivalent model of wind turbine generators (WTGs)

Extracting the equivalent model of wind turbine generators is an important aspect during the planning of large wind power plants and their stability studies. In this section, how to determine the parameters of the equivalent model of DCIG based wind turbines are explained. In this method, it is assumed that the disturbance in a bus identically affects the performance of all wind turbines. To determine the aggregated model parameters of a wind farm, the equivalent of electrical and mechanical sections of the wind farm should be obtained. The equivalent model of a wind farm considering N number of wind turbines are expressed below:

The equivalent parameters of the torsional system such as inertia constant (H_{eq}), shaft stiffness (K_{eq}) and damping coefficient (D_{eq}), respectively, are obtained in (19), (20) and (21). According to (19)-(21), the summation of the torsional system parameters of wind turbines indicate the equivalent wind turbine parameters.

$$H_{eq} = \sum_{k=1}^N H_k \quad (19)$$

$$K_{eq} = \sum_{k=1}^N K_k \quad (20)$$

$$D_{eq} = \sum_{k=1}^N D_k \quad (21)$$

Where k -index represents the k th wind turbine in a wind farm.

The equivalent capacity of the wind turbines (S_{eq}) is obtained from the summation of each wind turbine capacity

according to (22).

$$S_{eq} = \sum_{k=1}^N S_k \quad (22)$$

Where S_k is the rating capacity of the k th wind turbine.

The equivalent parameters of the double cage induction generator (X_{eq}) are obtained from (23).

$$X_{eq} = \sum_{k=1}^N \alpha_k X_k \quad (23)$$

Where, X_k is a parameter of k th generator and α_k is a factor, which is calculated from (24).

$$\alpha_k = S_k / \sum_{k=1}^N S_k \quad (24)$$

Also, the equivalent shunt capacitors (C_{geq}) at the terminal of the equivalent induction generator is calculated from (25).

$$C_{geq} = \sum_{k=1}^N C_{gk} \quad (25)$$

Where C_{gk} is the shunt capacitance at the k th generator terminal.

E. Complete system model

The differential equations describing different subsystems are linearized by Taylor expansion and linear state-space model of each subsystem is stated as (26)-(28) [11].

$$\dot{X}_T = A_{TT} X_T + A_{TG} X_G + B_T u_T \quad (26)$$

$$\dot{X}_G = A_{GT} X_T + A_{GG} X_G + A_{GN} X_N \quad (27)$$

$$\dot{X}_N = A_{NG} X_G + A_{NN} X_N + B_N u_N \quad (28)$$

Equations (26)-(28) represent the state space of the turbine generator mechanical system, induction generator electrical system, and transmission network, respectively. Where, A and B respectively, are the coefficients matrix of the state variables and input vectors and the subscripts T, G, and N are related to the turbine, generator, and network. In addition, X_T , X_G , and X_N , respectively, are the state variables vector of the turbine generator mechanical, induction generator, and transmission network subsystems and represent as (29)-(31). Also, u_T and u_N , respectively, are the input of the turbine generator mechanical and transmission network subsystems and represent as (31)-(32). In (29)-(33), Δ is a linearization symbol of equations.

$$X_T = [\Delta \omega_t, \Delta \delta_{tg}, \Delta \omega_g] \quad (29)$$

$$X_G = [\Delta I_{ds}, \Delta I_{qs}, \Delta I_{dr1}, \Delta I_{qr1}, \Delta I_{dr2}, \Delta I_{qr2}] \quad (30)$$

$$X_N = [\Delta V_{ds}, \Delta V_{qs}, \Delta I_d, \Delta I_q, \Delta V_{cd}, \Delta V_{cq}] \quad (31)$$

$$U_T = [\Delta T_\omega] \quad (32)$$

$$U_N = [\Delta V_{bd}, \Delta V_{bq}] \quad (33)$$

For every wind turbine, there is a set of equations (equations (1)-(11)). In the STR model, the wind farm is modeled by one equivalent wind turbine; therefore the wind

farm is modeled by 11 equations. The method for obtaining the equivalent wind turbine parameters is illustrated in section 3.4. In the MTR model, several wind turbine groups are considered, and each group of the wind turbine is modeled by the equivalent wind turbine. For example, if four groups of the wind turbine is considered the wind farm is modeled by 44 equations (the wind turbine in each group have the same electrical and mechanical parameters and is subjected to the same wind speed). In addition, in the FTR model, all of the wind turbines are modeled separately.

IV. SMALL SIGNAL ANALYSIS

In this section, in order to SSR analysis in a double-cage induction generator based wind farm connected to the series-compensated transmission line, the wind farm is modeled by three representations STR, MTR and FTR.

To comprehensive analysis of SSR, three scenarios are considered. In the first and second scenarios, all of the WTGs are identical but WTGs in the third scenario are different. In the first scenario, all wind turbines are subjected to the same wind speed (identical aerodynamic torque), and in the second scenario, each group of wind turbines is subjected to the same wind speed (wind speed is different between groups). In the third scenario, the electrical and mechanical parameters and also the capacity are different for each group of WTGs. The considered scenarios are summarized in Table I.

TABLE I

CONDITIONS CONSIDERED FOR WTGS IN DIFFERENT SCENARIOS		
Scenarios	Wind Speed	Electrical and Mechanical Parameters
Scenario 1	All wind turbines are subjected to the same wind speed	All wind turbines have the same electrical and mechanical parameters
Scenario 2	Each group of wind turbines is subjected to the same wind speed	All wind turbines have the same electrical and mechanical parameters
Scenario 3	Each group of wind turbines is subjected to the same wind speed	Each group of wind turbines has different electrical and mechanical parameters

In the following, for the mentioned scenarios, using linear modal analysis the eigenvalues of the benchmark system are calculated and compared for different wind farm representations. Since in this paper the effect of different wind farm representation on SSR phenomenon is studied; therefore, only the subsynchronous and torsional modes of the system are presented.

A. Small signal analysis of the Scenario 1

In the Scenario 1, a 101.2-MW wind farm is considered which consists of 44 double-cage IG-based wind turbines. In this scenario, all of the 44 generators are the same in terms of type (IG) and size (2.3 MW); and are subjected to identical aerodynamic torque ($T_w=1$ pu).

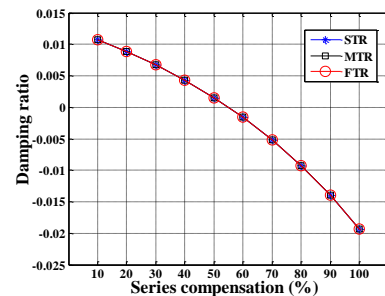
Table II shows the results of the small signal analysis for

different models of the wind farm and 50% series compensation level. In the MTR model, every 11 wind turbines are considered in one group. As shown in Table II, the results are the same for all three models. It should be noted that, in the STR model one torsional mode, and in the MTR and FTR, respectively, 4 and 44 torsional modes are obtained.

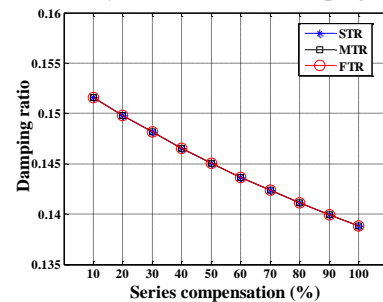
TABLE II
EIGENVALUES ASSOCIATED WITH SSR IN DIFFERENT REPRESENTATION MODELS FOR SCENARIO 1.

Modes Type	STR model	MTR model	FTR model
Subsynchronous mode	$-0.364 \pm j236.300$	$-0.364 \pm j236.300$	$-0.364 \pm j236.300$
Torsional mode(s)	$-0.527 \pm j3.594$	$-0.527 \pm j3.594$	$-0.527 \pm j3.594$

As shown in Table II, for this scenario, in MTR and FTR models, respectively, all 4 and 44 torsional modes are obtained as $-0.527 \pm j3.594$. For this scenario, the damping ratio variations of the subsynchronous and torsional modes for different series compensation levels are shown in Fig. 5. It should be noted that in the real power systems the compensation level is at a maximum of 75% range and higher values are meaningless (the normal compensation level is between 55% to 65%). According to Fig. 5, for Scenario 1, the damping ratio of these two modes is the same at all series compensation levels in all three models.



(a) Subsynchronous mode damping ratio



(b) Torsional mode damping ratio

Fig. 5. Subsynchronous and torsional modes damping ratio in different representation models for Scenario 1.

B. Small signal analysis of the Scenario 2

In the Scenario 2, same as Scenario 1, 44 identical wind turbines with 2.3 MW capacity are considered. But unlike the Scenario 1, different aerodynamic torques are applied to the wind turbines. 4 groups of 11 wind turbines (group A, group

B, group C and group D) are assumed that are subjected to the different aerodynamic torques (subjected to different wind speed). Group A produces rated output power ($T_w=1$ pu), group B produces 75% of its rated output power ($T_w=0.75$ pu), group C produces 50% of its rated output power ($T_w=0.5$ pu), and group D produces 25% of its rated output power ($T_w=0.25$ pu). Therefore, the generated power of the wind farm to be reduced to 63.25 MW.

The results of the small signal analysis of the Scenario 2 are presented in Table III for a 50% series compensation level and various wind farm models. As seen from Table III, in the STR model one torsional mode equal to $-0.341 \pm j236.268$ is obtained. In MTR model, 4 torsional modes equal to $-0.425 \pm j3.609$, $-0.434 \pm j3.608$, $-0.461 \pm j3.608$, and $-0.505 \pm j3.608$ are obtained that be associated with the 4 groups A, B, C, and D, respectively. In FTR model, 44 torsional modes are obtained such that 11 torsional modes are equal to $-0.425 \pm j3.609$, 11 torsional modes are equal to $-0.434 \pm j3.608$, 11 torsional modes are equal to $-0.461 \pm j3.608$, and 11 torsional modes are equal to $-0.505 \pm j3.608$.

TABLE III

EIGENVALUES ASSOCIATED WITH SSR IN DIFFERENT REPRESENTATION MODELS FOR SCENARIO 2.

Modes Type	STR model	MTR model	FTR model
Subsynchronous mode	$-0.341 \pm j236.268$	$-0.342 \pm j236.273$	$-0.342 \pm j236.273$
Torsional mode(s)		$-0.425 \pm j3.609$	$-0.425 \pm j3.609$
	$-0.447 \pm j3.594$	$-0.434 \pm j3.608$	$-0.434 \pm j3.608$
		$-0.461 \pm j3.608$	$-0.461 \pm j3.608$
		$-0.505 \pm j3.608$	$-0.505 \pm j3.608$

As shown in Table III, the subsynchronous mode is almost identical in all three models, but the torsional mode in the STR model is different from torsional modes obtained by MTR and FTR models. Also, the results of the MTR and FTR model are completely identical. In addition, the results show that when the mechanical parameters of wind turbines are the same, there is a negative correlation between wind turbine output power and torsional modes damping. Such that, in the MTR and FTR models, respectively, each group of wind turbines and each wind turbines that produce more power, has the least damping of torsional modes. Fig. 6 shows the damping ratio of the subsynchronous and the torsional modes for different series compensation levels in the Scenario 2.

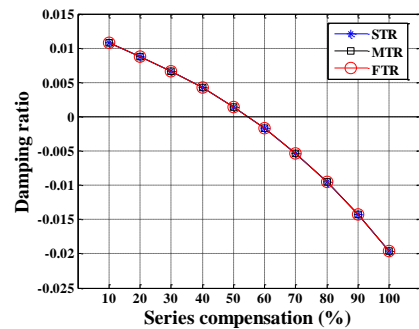
According to Fig. 6, the damping ratio of the subsynchronous mode is the same in all three models for the same series compensation levels, and the damping ratio of torsional modes are different for STR model than MTR and FTR models.

C. Small signal analysis of the Scenario 3

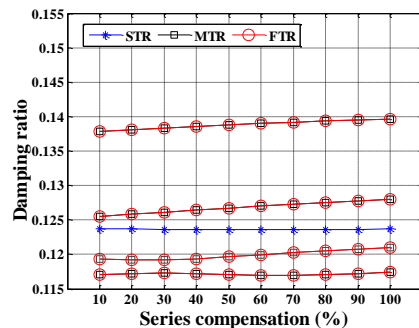
In the Scenario 3, a 112-MW wind farm is considered which includes wind turbine-generators by different electrical and mechanical parameters, and different output rated power.

For this purpose, 20 wind turbines with an induction generator of 2.3 MW, 20 wind turbines with an induction generator of 2 MW and 20 wind turbines with an induction generator of 1.3 MW are considered. In this scenario, it is assumed that each wind turbine produces the rated output power. In MTR model, the same wind turbine generators are modeled in the same group. Therefore, group A involves induction generators of 2.3 MW, group B involves induction generators of 2 MW and group C involves induction generators of 1.3 MW.

Table IV shows the system eigenvalues related to SSR in different representation models for Scenario 3. As seen from Table IV, in the STR model one torsional mode equal to $-0.429 \pm j3.392$ is obtained. In MTR model, 3 torsional modes equal to $-0.517 \pm j3.603$, $-0.265 \pm j2.516$ and $-0.434 \pm j4.579$ are obtained that be associated with the 3 groups A, B, and C, respectively. In FTR model, 60 torsional modes are obtained such that 20 torsional modes are equal to $-0.517 \pm j3.603$, 20 torsional modes are equal to $-0.265 \pm j2.516$, and 20 torsional modes are equal to $-0.434 \pm j4.579$.



(a) Subsynchronous mode damping ratio



(b) Torsional mode damping ratio

Fig. 6. Subsynchronous and torsional modes damping ratio in different representation models for Scenario 2.

TABLE IV

EIGENVALUES ASSOCIATED WITH SSR IN DIFFERENT REPRESENTATION MODELS FOR SCENARIO 3.

Modes Type	STR model	MTR model	FTR model
Subsynchronous mode	$-0.542 \pm j231.150$	$-0.571 \pm j231.121$	$-0.571 \pm j231.121$
Torsional mode(s)		$-0.517 \pm j3.603$	$-0.517 \pm j3.603$
	$-0.429 \pm j3.392$	$-0.265 \pm j2.516$	$-0.265 \pm j2.516$
		$-0.434 \pm j4.579$	$-0.434 \pm j4.579$

As seen from Table IV, the subsynchronous mode is close to each other in all three models, but the torsional mode in the STR model is different from torsional modes obtained by MTR and FTR models. Also, the results of the MTR and FTR model are completely identical. In addition, in this scenario, the wind turbines with an induction generator of 2 MW have the least damping of torsional modes. Fig. 7 shows the damping ratio of the subsynchronous and the torsional modes in different series compensation levels for the Scenario 3. As seen in Fig. 7, in the different representation of wind farm the damping ratio of the subsynchronous mode is the same in any series compensation levels; while that the damping ratio of torsional modes are different for STR model than MTR and FTR models.

With respect to the obtained results shown in Table II, Table III and Table IV, it is concluded when a wind farm includes of identical wind turbine-generators, and all of the wind turbines subject to the equal wind speed, the STR model is accurate for SSR analysis and there is no need for more complex model such that MTR and FTR models. But in the real condition of wind farms even the wind turbine-generators are identical, the wind turbines experienced different wind speeds. Therefore, the MTR, and FTR models should be used in SSR analysis. In addition, these results show that the FTR model of the wind farm can be replaced by MTR model in SSR analysis.

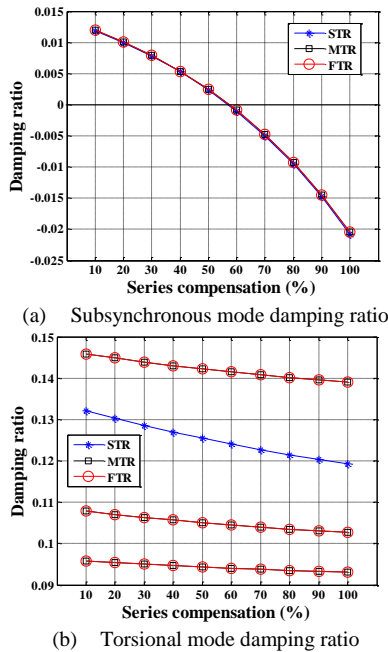


Fig. 7. Subsynchronous and torsional modes damping ratio in different representation models for Scenario 3.

V. SIMULATION

In this section, the simulation of the considered scenarios is done with PSCAD/EMTDC software to validate the small signal analysis. For system transient response, an LLLG fault

(three line to ground fault) occurs at the end of the transmission line (infinite bus) at $t=4$ seconds and lasts for six cycles (100ms). In order to obtain the frequency components of the electromagnetic and the shaft torques, Fast Fourier Transform (FFT) analysis is used. The simulation results are for 50% compensation level.

A. Simulation of the Scenario 1

The results of the Scenario 1 simulation are shown in Fig. 8 and Fig. 9. These figures, respectively, show the electromagnetic torque and the shaft torque with their frequency components. Simulation results are the same for all three models, moreover these results confirm stability and oscillation frequency of the small signal analysis results (Table II). Therefore, when the wind turbines and their output power are the same, all three models have the same results and the equivalent model (STR model) is suitable for SSR analysis in a wind farm with the same wind turbines and output powers.

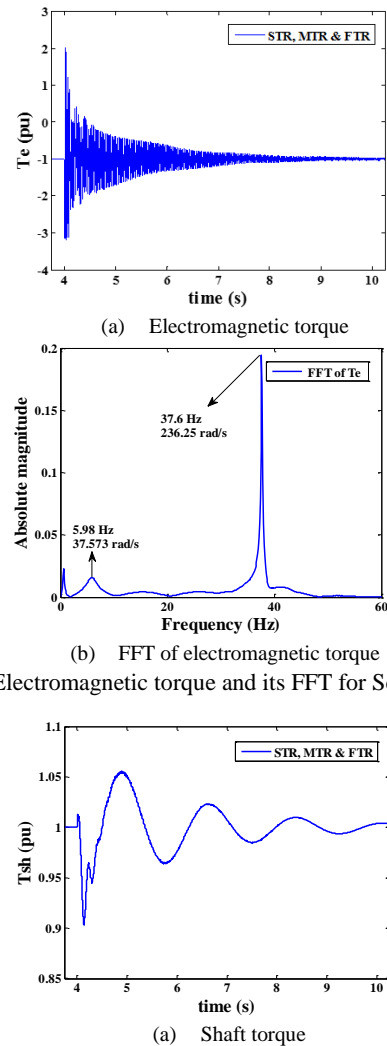
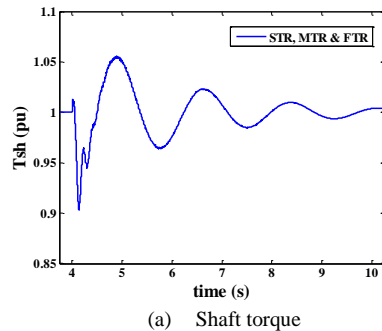


Fig. 8. Electromagnetic torque and its FFT for Scenario 1.



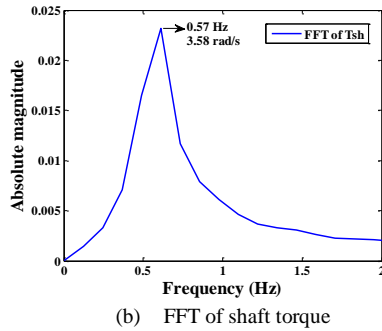


Fig. 9. Shaft torque and its FFT for Scenario 1.

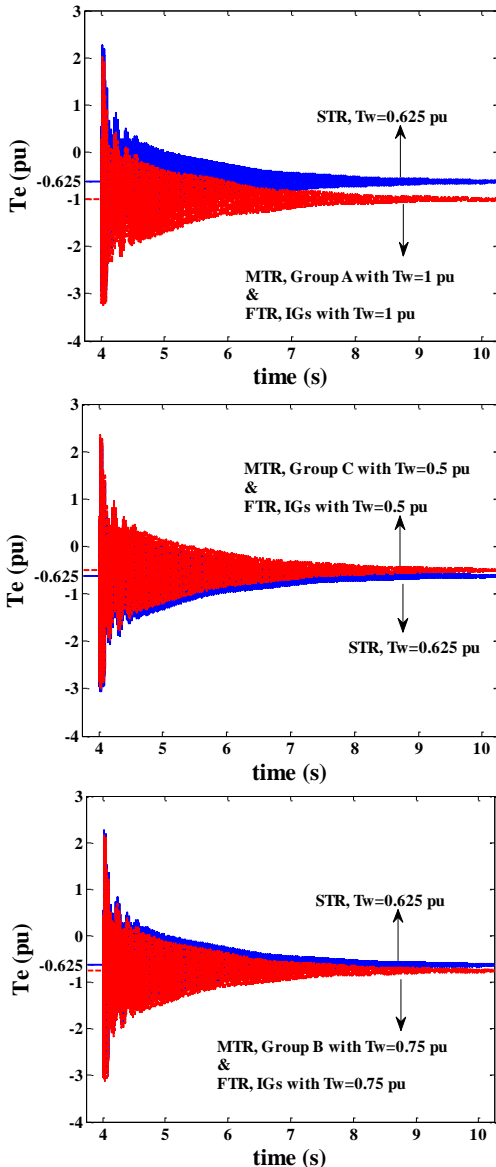


Fig. 10. Electromagnetic torques for Scenario 2.

B. Simulation of the Scenario 2

For Scenario 2, the generator electromagnetic torque in different wind farm models and their frequency components are shown in Fig. 10 and Fig. 11, respectively. As shown in Fig. 10, the transient behavior of the electromagnetic torque is the same in all models, and according to Fig. 11, the frequency and amplitude of the oscillations are the same in all three models.

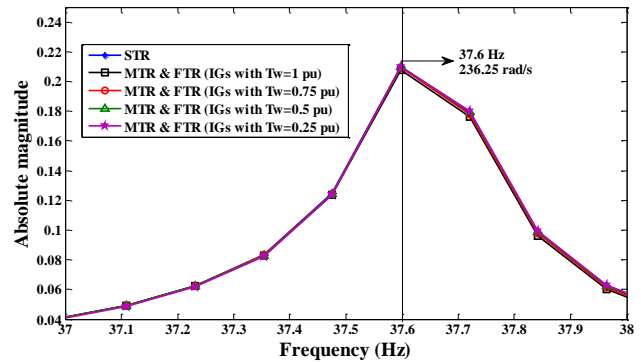


Fig. 11. FFT analysis of Electromagnetic torques for Scenario 2.

In Fig. 12, the torsional torques applied to the generator shaft and the FFT are shown for different models. Fig. 12 shows the torsional torques of the STR and the MTR models are different, while the MTR and FTR have completely similar results. Fig. 12 show that a group of wind turbines with a higher output power have higher torsional oscillations amplitude and less damping. Therefore, the results of simulation and small signal analysis show that in the SSR phenomenon analysis when wind turbines have different aerodynamic torques, the modeling of all wind turbines with an equivalent turbine (STR model) is not to be accurate enough. Also, the results show that using the exact model of wind turbines (FTR model) is not necessary, and the wind turbines with the same productive power can be modeled in the same group (MTR model).

C. Simulation of the Scenario 3

Fig. 13 and Fig. 14 respectively represent the electromagnetic torques for the different models of the wind farm for Scenario 3. Furthermore, the FFT analysis of this scenario is shown in Fig. 15. According to these two figures, the transient behavior in all three models, the amplitude and the frequency of the oscillations are the same and confirms the results of the small signal analysis (Table IV). Also, Fig. 16 shows the torques applied to the shaft of generators in different wind farm models and their FFT. According to Fig. 16, the transient behavior and the frequency of the torsional torques oscillations resulting from the simulation are

confirmed the small signal results. Fig. 16 shows that the MTR and FTR models have led to very similar results in determining the frequency and amplitude of the oscillations. While there is a little difference between the results of the STR model and the results of MTR and FTR models. Therefore, in a wind farm with different wind turbines for the SSR phenomenon analysis, the same wind turbines modeling in a group (MTR model) gives us more accurate results.

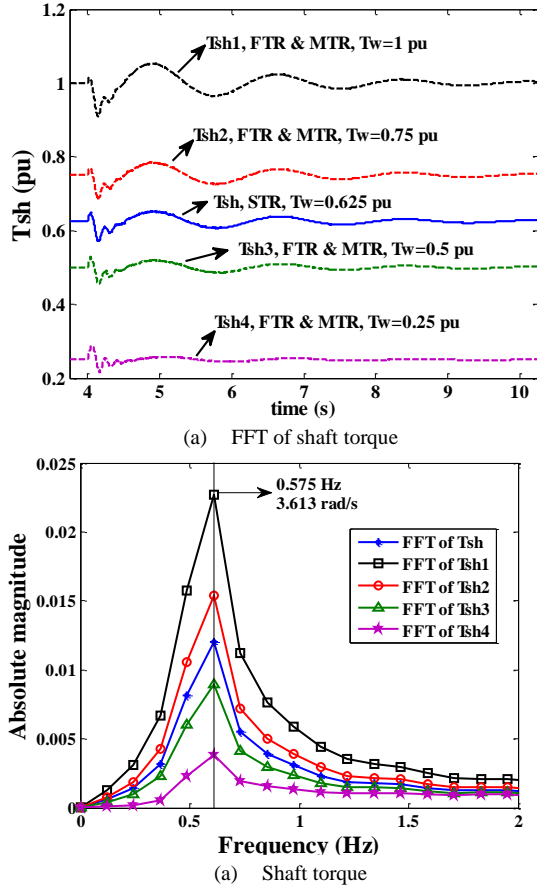


Fig. 12. Shaft torques and their FFT analysis for Scenario 2.

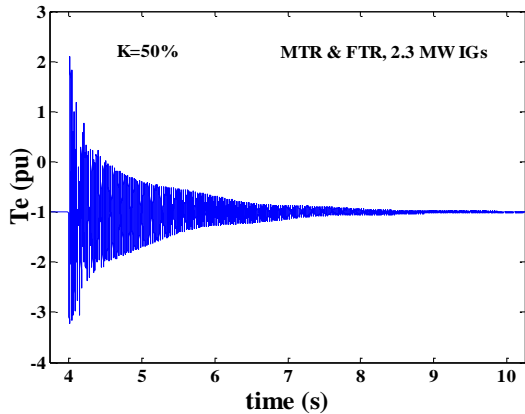


Fig. 13. Electromagnetic torques for STR model in Scenario 3.

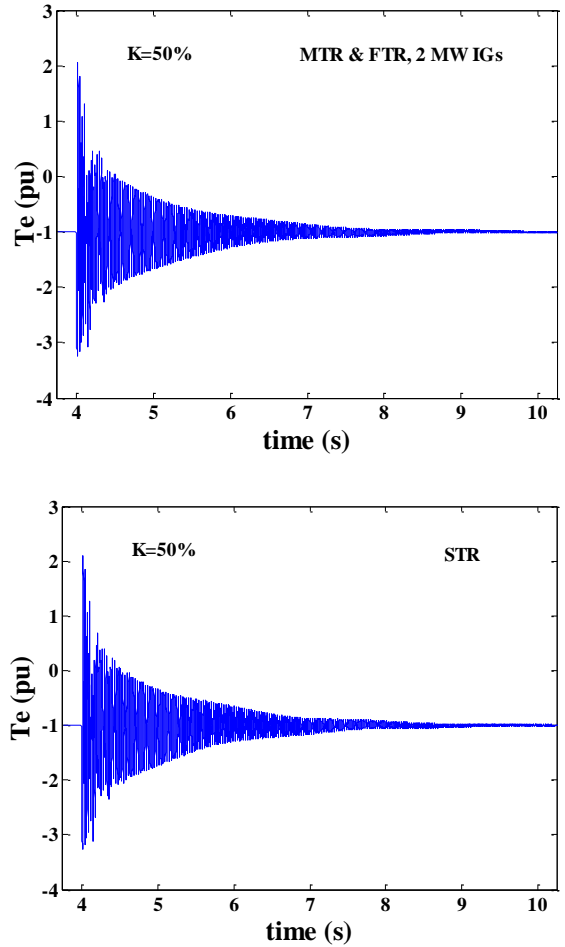


Fig. 14. Electromagnetic torques for MTR model in Scenario 3.

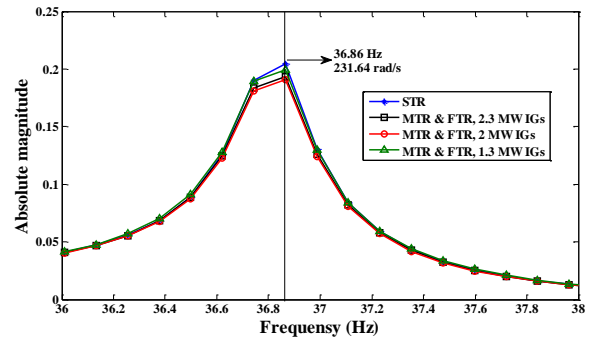


Fig. 15. FFT analysis of Electromagnetic torques for Scenario 3.

VI. CONCLUSIONS

In this paper, the effect of different representation types of wind turbines (STR, MTR and FTR models) on the SSR analysis in the double-cage IG based wind farm is studied. For this purpose, by the STR, MTR and FTR models both torsional interaction and induction generator effect are studied in different conditions of the power system. The results show that in all of these representation, the subsynchronous mode has not so much changed. Therefore, an equivalent model (STR model) for the wind farm is adequate to study the induction generator effect. Also, the increase in the series compensation level reduces the damping of this mode, and this mode becomes unstable from a series compensation level to next. Therefore, the induction generator effect is more influenced by the series compensation level and the different rated capacity and different output power of wind turbines has a little effect on the induction generator effect phenomenon. In addition, the increase in the series compensation level almost reduces the damping of torsional mode but this mode is stable for different series compensation levels. Furthermore, when all wind turbines are the same and affected by the same wind speed (the same aerodynamic torques), an equivalent model (STR model) is suitable for torsional interaction analysis. While that when wind turbines are subjected to different wind speed or the wind turbines are not the same in electrical and mechanical parameters, the STR model is not suitable to study the torsional interaction. In these conditions, the MTR model provides an accurate result of torsional interaction between the turbine generator and the series capacitor.

REFERENCES

- [1] A. Ackerman, *Wind power in power systems*, John Wiley and Sons, New York, 2005.
- [2] A. Lara, J. Ekanayake and C. Huges, *Wind energy generation modeling and control*, John Wiley and Sons, Chichester, U.K., 2009.
- [3] S. Sawyer, S. Teske and K. Rave, *Global wind energy outlook*, Available from: <http://www.gwec.net/>, 2014.
- [4] P. Ledesma and J. Usaola, "Transient stability of a fixed speed wind farm," *Renewable Energy*, Vol. 28, No. 9, pp. 1341-1355, 2003.
- [5] D. J. Trudnowski, A. Gentile, J. M. Khan and E. M. Petritz, "Fixed speed wind-generator and wind-park modeling for transient stability studies," *IEEE Transactions on Power Systems*, Vol. 19, No. 4, pp. 1911-1917, 2004.
- [6] E. Muljadi, C. Butterfield, B. Parsons and A. Ellis, "Effect of variable speed wind turbine generator on stability of a weak grid," *IEEE Transaction on Energy Conversion*, Vol. 22, No. 1, pp. 29-36, 2007.
- [7] A. Khajeh and Z. Shabani, "Adaptive gain scheduling control of doubly fed induction generator based wind turbines to improve fault ride through performance," *International Journal of Industrial Electronics, Control and Optimization*, Vol. 1, No. 1, pp. 61-70, 2018.
- [8] I. Erlich, J. Kretschmann, Fortmann, S. Mueller-Engelhardt and H. Wrede, "Modeling of wind turbines based on doubly-fed induction generators for power system stability studies," *IEEE Transactions on Power Systems*, Vol. 22, No. 3, pp. 909-919, 2007.
- [9] E. L. Petersen and P. H. Madsen, "wind Farms," *Encyclopedia of the Anthropocene*, Vol. 1, pp. 407-420, 2018.
- [10] A. Moharana and R. K. Varma, "Subsynchronous resonance in single cage self excited induction generator based wind farm connected to series-compensated lines," *IET Generation, Transmission & Distribution*, Vol. 5, No. 12, pp. 1221-1232, 2011.

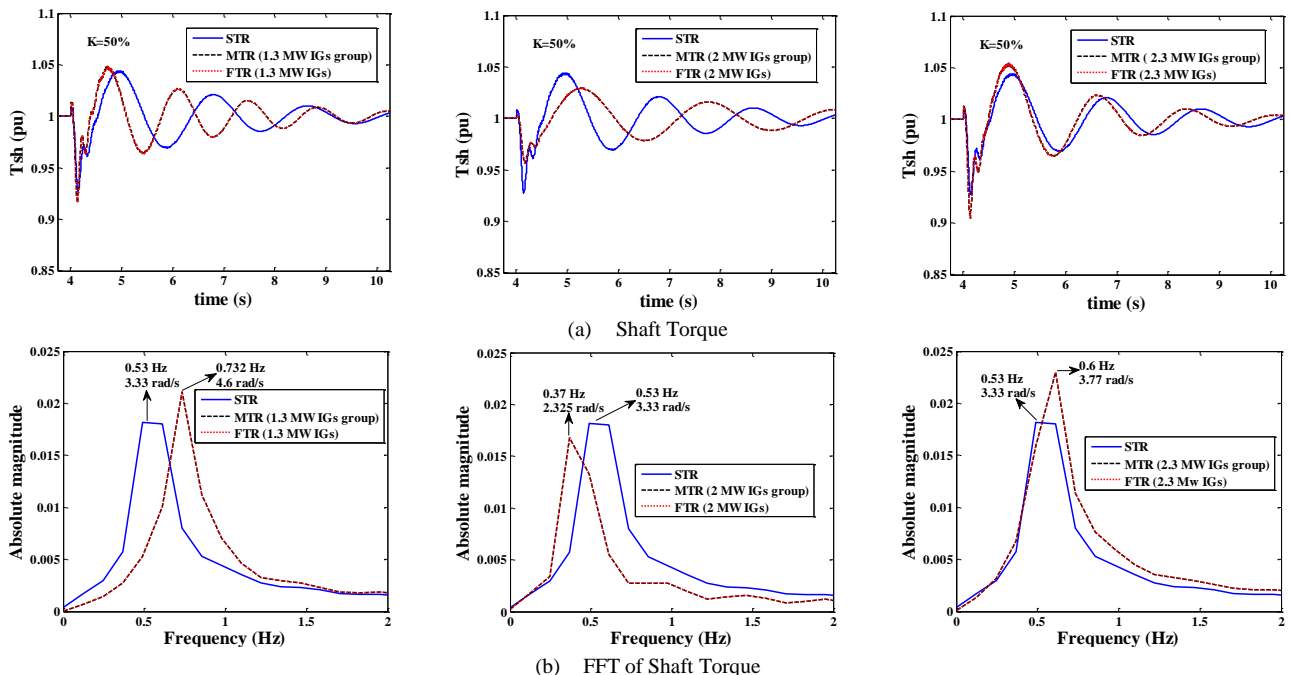


Fig. 16. Shaft torques and their FFT analysis for Scenario 3.

- [11] A. Moharana and R. K. Varma, "SSR in double-cage induction-generator-based wind farm connected to series-compensated Transmission line," *IEEE Transactions on Power Systems*, Vol. 28, No. 3, pp. 2573-2583, 2013.
- [12] M. Henderson, D. Bertagnolli and D. Ramey, "Planning HVDC and FACTS in New England," *Proc. IEEE/PES PSCE*, Seattle, WA, USA, pp. 1-3, 15-18 March 2009.
- [13] P. Kundur, *Power system stability and control*, Tata McGraw-Hill, New York, 1994.
- [14] K. Padiyar, *Analysis of subsynchronous resonance in power system*, Kluwer Academic, 1999.
- [15] A. Tabesh and R. Iravani, "Small-signal dynamic model and analysis of a fixed-speed wind farm—A frequency response approach," *IEEE Transaction on Power Delivery*, Vol. 21, No. 2, pp. 778–787, 2006.
- [16] S. M. Chan, R. L. Cresap and D. H. Curtice, "Wind turbine cluster model," *IEEE Transactions on Power Apparatus and Systems*, Vol. 103, No. 7, pp. 1692–1698, 1984.
- [17] J. Xu, P. K. Kanyingi, K. Wang, G. Li and X. Jiang, "Probabilistic small signal stability analysis with large scale integration of wind power considering dependence," *Renewable and Sustainable Energy Reviews*, Vol. 69, pp. 1258-1270, 2017.
- [18] A. Ostadi, A. Yazdani and R. K. Varma, "Modeling and stability analysis of a DFIG-based wind-power generator interfaced with a series-compensated line," *IEEE Transaction on Power Delivery*, Vol. 24, No. 3, pp. 1504-1514, 2009.
- [19] L. Fan, C. Zhu, Z. Miao and M. Hu, "Modal analysis of a DFIG-based wind farm interfaced with a series compensated network," *IEEE Transaction on Energy Conversion*, Vol. 26, No. 4, pp. 1010-1020, 2011.
- [20] H. A. Mohammadpour and E. Santi, "Subsynchronous resonance analysis in DFIG-based wind farms: Definitions and problem identification — Part I," *Proceeding on IEEE Energy Conversion Congress and Exposition (ECCE)*, Pittsburgh, P.A., U.S.A., pp. 812-819, 14-18 September 2014.
- [21] A. Moharana, R. K. Varma, 'SSR alleviation by STATCOM in induction-generator-based wind farm connected to series compensated line,' *IEEE Transactions on Sustainable Energy*, Vol. 5, No. 3, pp. 947-957, 2014.
- [22] X. Xi, H. Geng and G. Yang, "Enhanced model of the doubly fed induction generator-based wind farm for small-signal stability studies of weak power system," *IET Renewable Power Generation*, Vol. 8, No. 7, pp. 765-774, 2014.
- [23] H. A. Mohammadpour, A. Ghaderi, and E. Santi, "Analysis of subsynchronous resonance in doubly-fed induction generator-based wind farms interfaced with gate – controlled series capacitor," *IET Generation, Transmission & Distribution*, Vol. 8, No. 12, pp. 1998-2011, 2014.
- [24] A. E. Leon, J. M. Mauricio and J. A. Solsona, "Subsynchronous resonance mitigation using variable speed wind energy conversion systems," *IET Generation, Transmission & Distribution*, Vol. 7, No. 5, pp. 511-525, 2013.
- [25] H. A. Mohammadpour, A. Ghaderi, H. Mohammadpour and E. Santi, "SSR damping in wind farms using observed-state feedback control of DFIG converters," *Electric Power Systems Research*, Vol. 123, PP. 57-66, 2015.
- [26] F. Mancilla-David, J. L. Domínguez-García, M. De Prada, O. Gomis-Bellmunt, M. Singh and E. Muljadi, "Modeling and control of Type-2 wind turbines for subsynchronous resonance damping," *Energy Conversion and Management*, Vol. 97, pp. 315-322, 2015.
- [27] A. Vassel-Be-Hagh, C. L. Archer, "Wind farms with counter-rotating wind turbines," *Sustainable Energy Technologies and Assessments*, Vol. 24, pp. 19-30, 2017.
- [28] V. B. Virulkar and G.V. Gotmare, "Subsynchronous resonance in series compensated wind farm: a review," *Renewable and Sustainable Energy Reviews*, Vol. 55, pp. 1010-1029, 2016.
- [29] X. Xie, X. Zhang, H. Liu, Y. Li, and C. Zhang, "Characteristic analysis of subsynchronous resonance in practical wind farms connected to series-compensated transmissions," *IEEE Transaction on Energy Conversion*, Vol. 32, No. 3, pp. 1117-1126, 2017.
- [30] X. Zhang, X. Xie, H. Liu, H. and Y. Li, "Mitigation of subsynchronous control interaction in wind power systems with GA-SA tuned damping controller," *IFAC Papers Online*, Vol. 50, No. 1, pp. 8740–8745, 2017.
- [31] S. Chernet, M. Beza and M. Bongiorno, "Investigation of subsynchronous control interaction in DFIG-based wind farms connected to a series compensated transmission line," *Electrical Power and Energy Systems*, Vol. 105, pp. 765-774, 2019.
- [32] L. Shi and G. Xu, "Subsynchronous resonance analysis and simulation on wind farm," *2nd International Conference on Power and Renewable Energy (ICPRE)*, pp. 412-416, 2017.
- [33] B. Zoghdar-Moghadam-Shahrekohne and S. M. Barakati, "A novel approach for mitigating SSR in DFIG-based wind farms integrated into series compensated network," *9th International Congress on Ultra Modern Telecommunications and Control Systems and Workshops (ICUMT)*, Munich, pp. 311-317, 2017.
- [34] W. Chen, X. Xie, D. Wang, H. Liu and H. Liu, "Probabilistic Stability Analysis of Subsynchronous Resonance for Series-Compensated DFIG Based Wind Farms," *IEEE Transactions on Sustainable Energy*, Vol. 9, No. 1, pp. 400-409, 2018.
- [35] J. Shaira, X. Xie, L. Wang, W. Liu, J. He, and H. Liu, "Overview of emerging subsynchronous oscillations in practical wind power systems," *Renewable and Sustainable Energy Reviews*, Vol. 99, pp. 159–168, 2019.
- [36] A. K. Moharana, Subsynchronous resonance in wind farms, Ph.D. Thesis, Dept. of ECE, University of Western Ontario, Canada, 2012.
- [37] P. C. Krause, O. Wasynczuk, and S. D. Sudho, *Analysis of Electric Machinery and Drive Systems*, IEEE Press, 2002.

APPENDIX

TABLE V
DOUBLE-CAGE INDUCTION GENERATORS DATA.

Parameter	2.3 MW IG	2 MW IG	1.3 MW IG
P	2.3 MW	2 MW	1.3 MW
V	690 V	690 V	690 V
F	60 Hz	60 Hz	60 Hz
Number of poles	6	6	6

CONTINUED. TABLE V

R_s (pu)	0.00506	0.00506	0.0074
X_{so} (pu)	0.13176	0.12552	0.1485
R_{r1} (pu)	0.01199	0.01165	0.0129
R_{r2} (pu)	0.019239	0.018624	0.0124
$X_{r\sigma 1}$ (pu)	0	0	0
$X_{r\sigma 2}$ (pu)	0.21172	0.28565	0.1345
X_{rm} (pu)	0.072175	0.078995	0.0499
X_m (pu)	3.8892	4.00508	4.369



Mohamad Kazem Salehi was born in Shahrabak, Iran. He received his M.Sc. Degrees in electrical engineering from Graduate University of Advanced Technology, Kerman, Iran, in 2016. His research interests include application of power electronics in power systems, renewable energy, and wind power plants. He is currently PhD student of electrical engineering in Shiraz University of Technology, Shiraz, Iran.



Roohalamin Zeinali Davarani was born in Rafsanjan, Iran. He received the B.Sc. degree from Shahid Bahonar University of Kerman, Kerman, Iran, in 2004. He obtained the M.Sc. and PhD degrees from Ferdowsi University of Mashhad, Mashhad, Iran, respectively in 2007 and 2012, all in electrical engineering. He is currently assistant professor of electrical engineering in Graduate University of Advanced Technology, Kerman, Iran. His research interests include power system dynamic and control, renewable energies, and FACTS devices.

TABLE VI
TRANSMISSION LINE DATA

Parameter	Value	Parameter	Value
System Base Voltage	892.4 MVA	R	0.02 pu
	500 kV	X_b	0.06 pu
X_t	0.14 pu	X_c	(10% - 100%) ($X_t + X_L + X_b$)
X_L	0.50 pu		

TABLE VII
WIND TURBINES DATA.

Parameter	2.3 MW WT	2 MW WT	1.3 MW WT
Inertia constant of the wind turbine	4 s	4.29 s	2.5 s
Shaft stiffness	0.3 pu	0.15 pu	0.3 pu
Inertia constant of the generator	0.5 s	0.9 s	0.5 s
Damping coefficient	0 pu	0 pu	0 pu
Number of the blades	3	3	3
Rotor diameter	92 m	80 m	62.4 m
mechanical speed	1200 rpm	1200 rpm	1200 rpm
Angular speed of rotor	11 rpm	13.5 rpm	20 rpm
Gearbox ratio	109	88.8	60
Air density	1.225 kg/m ³	1.225 kg/m ³	1.225 kg/m ³

TABLE VIII
COLLECTOR CABLE DATA [Ω /M].

Resistance	Reactance
0.00046	0.000368